Neuroradiology
DOI 10.1007/s00234-007-0268-3

HEAD AND NECK RADIOLOGY

The value of single-shot turbo spin-echo diffusion-weighted MR imaging in the detection of middle ear cholesteatoma

Bert De Foer · Jean-Philippe Vercruysse · Anja Bernaerts · Joachim Maes · Filip Deckers · Johan Michiels · Thomas Somers · Marc Pouillon · Erwin Offeciers · Jan W. Casselman

Received: 3 May 2007 / Accepted: 4 June 2007

Abstract
Introduction Single-shot (SS) turbo spin-echo (TSE) diffusion-weighted (DW) magnetic resonance imaging (MRI) is a non echo-planar imaging (EPI) technique recently reported for the evaluation of middle ear cholesteatoma. We prospectively evaluated a SS TSE DW sequence in detecting congenital or acquired middle ear cholesteatoma and evaluated the size of middle ear cholesteatoma detectable with this sequence. The aim of this study was not to differentiate between inflammatory tissue and cholesteatoma using SS TSE DW imaging.
Methods A group of 21 patients strongly suspected clinically and/or otoscopically of having a middle ear cholesteatoma without any history of prior surgery were evaluated with late post-gadolinium MRI including this SS TSE DW sequence.
Results A total of 21 middle ear cholesteatomas (5 congenital and 16 acquired) were found at surgery with a size varying between 2 and 19 mm. Hyperintense signal on SS TSE DW imaging compatible with cholesteatoma was found in 19 patients. One patient showed no hyperintensity due to autoevacuation of the cholesteatoma sac into the external auditory canal. Another patient showed no hyperintensity because of motion artifacts.
Conclusion This study shows the high sensitivity of this SS TSE DW sequence in detecting small middle ear cholesteatomas, with a size limit as small as 2 mm.

Keywords Cholesteatoma · Diffusion · DWI · MR

B. De Foer (✉) · A. Bernaerts · J. Maes · F. Deckers · M. Pouillon · J. W. Casselman
Department of Radiology, A.Z. Sint-Augustinus Hospital, Antwerp, Belgium
e-mail: bert.defoer@GZA.be

J.-P. Vercruysse · T. Somers · E. Offeciers
University Department of ENT, A.Z. Sint-Augustinus Hospital, Antwerp, Belgium

J. W. Casselman
Department of Radiology, A.Z. Sint-Jan AV, Bruges, Belgium

J. Michiels
Siemens Medical Solutions, Anderlecht, Belgium

Introduction

In the detection and description of the extension of a suspected middle ear cholesteatoma, CT is still considered the imaging method of choice. It can demonstrate ossicular erosion and possible complications such as tegmental disruption and fistulization through the lateral semicircular canal. In the past few years, magnetic resonance (MR) imaging, including diffusion-weighted (DW) echo-planar imaging (EPI), has gained increasing importance in the detection of acquired middle ear cholesteatoma [1, 2].

DW EPI has been shown to be accurate in differentiating inflammatory tissue from cholesteatoma in the non-surgically treated middle ear, as cholesteatoma demonstrates a clear hyperintensity on DW EPI sequences in contrast to inflammatory tissue [1].

Several reports have discussed the value of DW EPI [2] and late post-gadolinium T1-weighted sequences [3, 4] in the detection of pre-second-look residual cholesteatoma and postoperative recurrent cholesteatoma [5–7]. DW EPI, however, fails to demonstrate middle ear cholesteatoma with a size smaller than 5 mm due to susceptibility artifacts, lower imaging matrix and relatively thick slices [2, 7]. Recent reports have highlighted the use and value of a non-

EPI-based DW sequence in the diagnosis of primary middle ear cholesteatoma [8] and postoperative recurrent cholesteatoma [9]. The purpose of this study was to evaluate the sensitivity of a single-shot (SS) turbo spin-echo (TSE) DW sequence in detecting middle ear cholesteatoma and more specifically to evaluate the size of middle ear cholesteatoma detectable with a SS TSE DW MR imaging sequence compared to the 5 mm size limit of the commonly used DW EPI.

Materials and methods

Patients

Between 2 August 2005 and 12 December 2006, we evaluated 21 patients strongly suspected clinically and/or otoscopically of having a middle ear cholesteatoma, prior to their planned surgery. We used the combination of late post-gadolinium coronal and axial T1-weighted sequences and a SS TSE DW sequence. In five patients, a DW EPI sequence was also performed. Prior to MR imaging examination, all but one patient had a CT scan as part of their preoperative work-up. All patients were operated upon within 4 months of MR imaging. The patients consisted of 4 women and 17 men with an average age of 36 years. Cholesteatoma surgery was performed by one of two experienced surgeons (T.S. or E.O.). The surgical findings, including the exact location of the cholesteatoma, were obtained from surgical reports and discussion with the surgeon.

Imaging technique

CT was performed on a 16-row multislice scanner (Lightspeed, GE, Milwaukee, Wis.) using an axial volume scan (140 kV, 250 mA, 1-s rotation, 5.62 pitch, high resolution bone algorithm) with coronal reformations. Axial slices were acquired at a thickness of 0.625 mm, centered in a 9.6-cm field of view on the right and left ear, with a reconstruction interval of 0.2 mm. MR imaging was performed on a 1.5-T superconductive unit (Magnetom Avanto, Siemens Medical Solutions, Erlangen, Germany) using the standard head matrix coil and two 7-cm surface ring coils. Axial 2-mm thick spin-echo (SE) T1-weighted images were obtained with the following parameters: TR 400 ms, TE 17 ms, matrix 192×256, field of view 150×200 mm, two averages, acquisition time 3 min 50 s. Coronal 2-mm thick SE T1-weighted images were acquired with the same parameters except for the matrix, which was set at 144×256. Coronal 2-mm thick TSE T2-weighted images (TR 3,500 ms, TE 92 ms, matrix 192×256, field of view 150×200 mm, turbofactor 13, 12 sections, two averages, acquisition time 2 min 41 s) and axial 0.4 mm thick 3-D TSE T2-weighted images (TR 1,500 ms, TE 303 ms, matrix 228×448, field of view 107×210 mm, turbofactor 37, 48 sections, one average, acquisition time 6 min 19 s) were also obtained. In all patients, 2 mm thick SS TSE DW images were acquired in the coronal plane (TR 2,000 ms, TE 115 ms, matrix 134×192, field of view 220×220 mm, b 0 and 1,000 mm^2/s ten signals acquired, 12 sections, imaging time 4 min 2 s). In five patients, 3 mm thick SE planar DW images were also acquired (TR 3,000, TE 82, matrix 128×128, field of view 210×210 mm, b 0 and 1,000 mm^2/s, 20 sections, six signals acquired, imaging time 2 min 14 s). Parallel imaging techniques were not used. All images were acquired 45 min after intravenous injection of 0.1 mmol per kg of body weight gadoterate meglumine (Dotarem, Guerbet, Roissy, France) or gadopentetate dimeglumine (Magnevist, Schering, Berlin, Germany).

Image interpretation

All images were prospectively interpreted by two radiologists experienced in head and neck radiology (J.W.C. and A.B. with 15 and 3 years of experience, respectively, in MR imaging of the middle ear). Both radiologists were blinded to the patients' identity, clinical data and CT data. Available DW EPI were scored first. The degree of distortion was noted. Then, all SS TSE DW images were scored by both readers. The findings on SS TSE DW images were correlated with standard T1- and T2-weighted MR images, in order to determine the degree of correlation and to exactly localize the lesion. We were able to calculate ADC maps in 12 cases. On DW EPI as well as on SS TSE DW images, cholesteatoma was diagnosed if a marked hyperintensity in comparison with brain tissue (b 1,000) was found. Standard MR imaging sequences were evaluated looking for a moderately hyperintense lesion on T2-weighted images, the characteristic peripheral enhancing cholesteatoma matrix and the central nonenhancing cholesteatoma on T1-weighted images. The size of the lesion was measured at its maximum transverse diameter on both axial and coronal delayed contrast-enhanced T1-weighted SE images. All cases were classified as positive or negative, according to the signal characteristics described above. Welch's test (F-test 0.045) was used to determine the significance of differences in the ADC values between cholesteatoma and gray matter of adjacent temporal bone.

Results

At surgery, 21 middle ear cholesteatomas were found, of which 5 were considered congenital and 16 acquired (Table 1). The size and location of the cholesteatomas as determined by MR imaging were in agreement with those

Table 1 Identification of cholesteatomas on MR imaging

Patient no.	Gender	Side	Congenital/acquired	Size (mm)	EPI DW imaging		SS TSE DW imaging		T2-W and delayed T1-W imaging[a]		ADC (mm^2/s) × 10^{-6}	
					Reader 1	Reader 2	Reader 1	Reader 2	Reader 1	Reader 2	Cholesteatoma	Brain
1	F	Left	Congenital	2	NA	NA	+	+	−	+ (only T2)	NA	NA
2	M	Left	Congenital	8	NA	NA	+	+	+	+	NA	NA
3	M	Left	Acquired	2	−	−	+	+	+	+	NA	NA
4	F	Left	Acquired	15	NA	NA	+	+	+	+	NA	NA
5	M	Left	Acquired	8	NA	NA	+	+	+	+	NA	NA
6	M	Left	Acquired	5	−	−	+	+	+	+	NA	NA
7	M	Left	Congenital	13	+ (distortion)	+ (distortion)	+	+	+	+	74	79
8	M	Right	Acquired	Autoevacuated	NA	NA	−	−	−	−	NA	NA
9	M	Left	Acquired	10	+	+	+	+	+	+	72	86
10	M	Left	Acquired	4	−	−	+	+	−	+	82	96
11	M	Left	Acquired	3	NA	NA	+	+	+	+	67	82
12	M	Left	Acquired	10	NA	NA	+	+	+	+	80	79
13	F	Right	Acquired	9	NA	NA	+	+	+	+	74	80
14	M	Right	Congenital	5	NA	NA	+	+	+	+	60	80
15	F	Left	Acquired	12	NA	NA	+	+	+	+	88	72
16	M	Left	Acquired	5	NA	NA	+	+	+	+	86	75
17	M	Right	Acquired	12	NA	NA	+	+	+	+	59	79
18	M	Left	Acquired	19	NA	NA	+	+	+	+	77	82
19	M	Right	Acquired	6	NA	NA	+	+	+	+	98	94
20	M	Left	Acquired	3	NA	NA	+	+	+	+	NA	NA
21	M	Right	Congenital	3	NA	NA	−	−	−	+	NA	NA

[a] Delayed T1-W imaging: T1-weighted MR imaging sequence performed 45 min after intravenous administration of gadolinium.
NA, Non applicable

found at surgery. The lesion size varied between 2 and 19 mm. There were two false-negative cases on the SS TSE DW images. One of the false-negative cases (considered negative by both readers on SS TSE DW as well as on T2-weighted and late post-gadolinium T1-weighted MR images) was a cholesteatoma sac that had autoevacuated into the external auditory canal (patient 8) (Fig. 1).

The other false-negative case considered to be negative on SS TSE DW images by both readers was a 3-mm epitympanic congenital cholesteatoma in a young child (patient 21). This examination was degraded by motion artifacts in all sequences, with no clear hyperintensity seen on SS TSE DW images. However, the cholesteatoma in this patient was diagnosed by one of the readers on standard late post-gadolinium T1-weighted sequences as well as on T2-weighted sequences (Fig. 2). All 19 other patients showed a nodular hyperintensity on SS TSE DW images, diagnosed as such by both readers. The size of the smallest cholesteatoma was 2 mm (Fig. 3; patients 1 and 3). Disagreement was seen between the interpretations of the two radiologists on the standard T2-weighted and late post-gadolinium images in two of these 19 patients (patients 1 and 10). In these patients both readers interpreted the SS TSE DW images as positive, but reader 1 failed to recognize the cholesteatoma on standard T2-weighted and late-post gadolinium T1-weighted MR images. No susceptibility artifacts were present on this patient's SS TSE DW images. In five patients, DW EPI was also performed. In two of these findings of cholesteatoma, measuring 10 and 13 mm, respectively (patients 7 and 9), were interpreted as positive on DW EPI images by both readers (Fig. 4). All other DW EPI images were interpreted as negative by both readers, but in these particular three patients they were interpreted as positive on SS TSE DW images (patients 3, 6 and 10). ADC maps were calculated for 12 patients (Table 1). In these 12 patients, there was no statistically significant difference in the ADC value of the cholesteatoma and the gray matter of the adjacent temporal lobe ($P > 0.05$). For all other patients, ADC maps could not be calculated because of technical limitations or the small size of the lesion.

Discussion

CT still remains the first imaging tool for diagnosis, description of extension and possible complications of middle ear cholesteatoma. However, in the presence of associated complications, MR imaging clearly has an additional role [10]. Several reports have stressed the role of DW EPI in the diagnosis of middle ear cholesteatoma [1, 2], evaluation of pre-second-look residual cholesteatoma [2] and recurrent or relapsing cholesteatoma [5–7]. DW EPI has been shown to be accurate in differentiating inflamma-

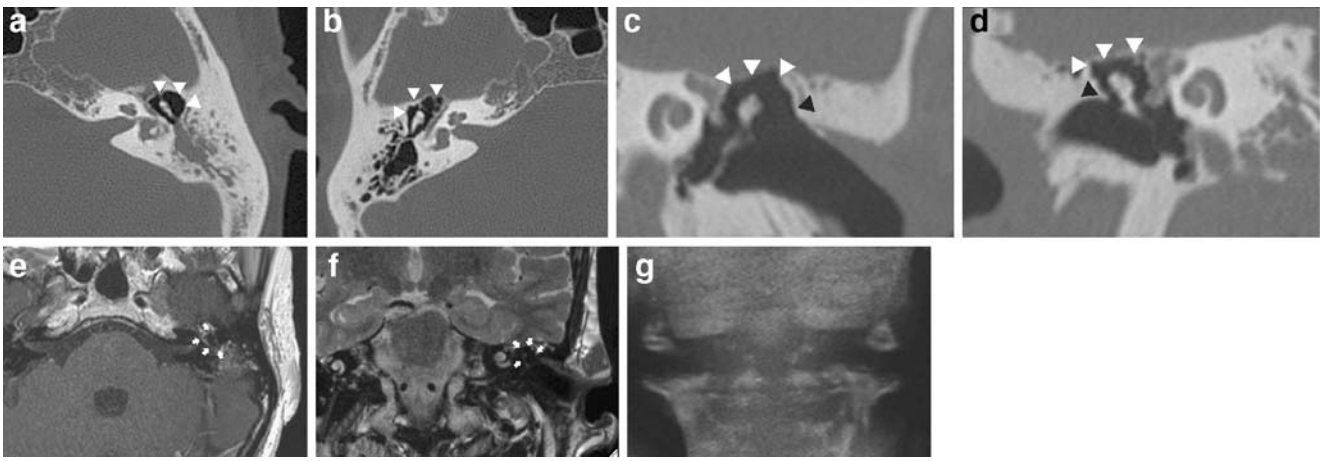

Fig. 1 Patient 8: cholesteatoma autoevacuated into the external auditory canal on the left side. **a** Axial CT image on the left side at the level of the epitympanon showing an eroded lateral epitympanic wall (*arrowheads*). Note that the malleus and incus look eroded and "thinned" in their laterolateral diameter. Compare with the normal situation in **b**. The cholesteatoma has eroded the lateral epitympanic wall and the ossicular chain. The associated soft tissue lesion typically seen in such cases is not visible due to its evacuation into the external auditory canal. **b** Axial CT image on the right side (same level as **a**) showing the normal distance of the ossicular chain to the lateral epitympanic wall (*arrowheads*). Note the normal aspect of the ossicular chain. Compare with the abnormal aspect of the lateral epitympanic wall and ossicular chain in **a**. **c** Coronal CT reformation at the level of the cochlea on the left side showing the empty cholesteatoma sac (*white arrowheads*) causing an eroded aspect of the head of the malleus and an amputated scutum (*black arrowhead*). Again, there is no soft tissue visible. Compare with the normal right side in **d**. **d** Coronal CT reformation at the level of the cochlea on the right side showing a normal epitympanic space (*white arrowheads*), normal ossicular chain and a normal scutum (*black arrowhead*). **e** Axial late T1-weighted MR image after gadolinium administration at the level of the epitympanon (same level as **a**) showing the enhancing inflammation and cholesteatoma matrix (*arrows*) around the evacuated air-filled cholesteatoma sac. **f** Coronal T2-weighted MR image at the level of the cochlea (same level as **c**) showing the hypointense air-filled empty cholesteatoma sac (*arrows*). **g** Coronal SS TSE DW image (same level as **c** and **f**) showing no clear hyperintensity

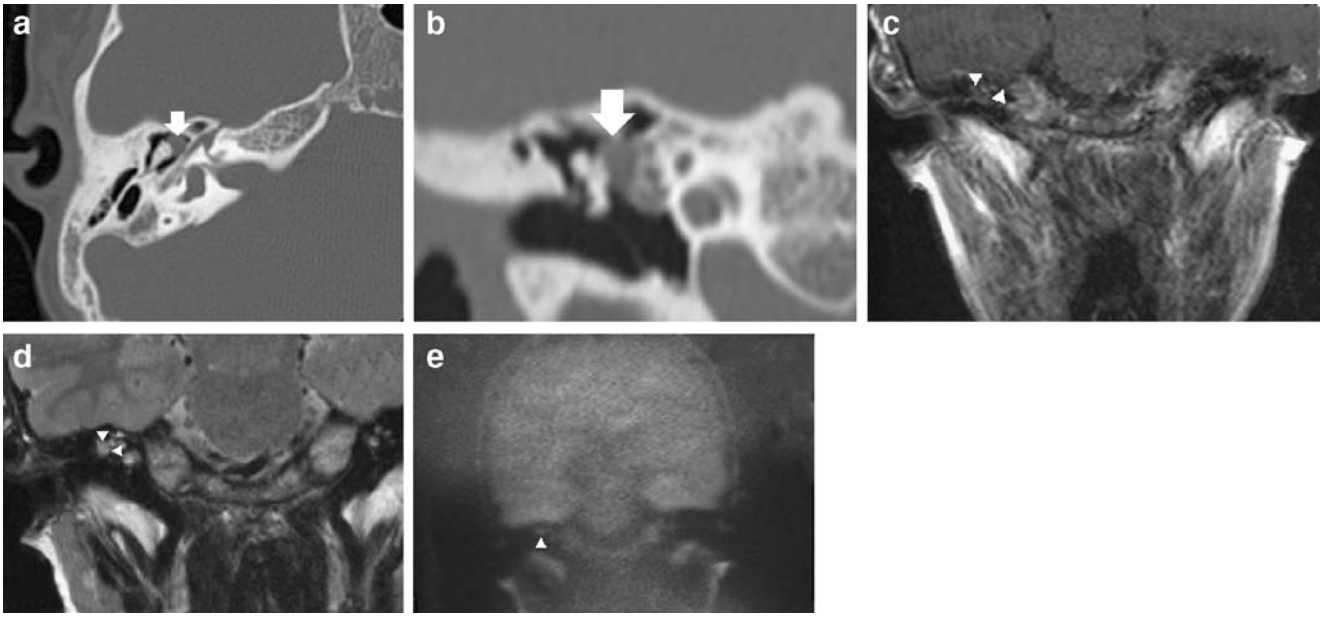

Fig. 2 Patient 21: small (3 mm) congenital epitympanic cholesteatoma in a young child. Examination degraded by motion artifacts. **a** Axial CT image at the level of the head of the malleus and incus body showing a small nodular soft tissue lesion (*arrow*) protruding into the anterior epitympanic recessus. **b** Coronal reformation at the level of the anterior epitympanic recessus showing a small nodular soft tissue lesion (*arrow*) eroding the malleus head. **c** Coronal late post-gadolinium T1-weighted MR image degraded by motion artifacts at the level of the anterior epitympanic recessus (same level as **b**) showing a hypointense lesion (*arrowheads*) surrounded by enhancing inflammation: small nonenhancing cholesteatoma surrounded by enhancing inflammation. **d** Coronal T2-weighted image degraded by motion artifacts at the level of the anterior epitympanic recessus (same level as **b** and **c**) showing a nodular moderate hyperintense lesion compatible with the small congenital cholesteatoma. **e** Coronal SS TSE DW image at the level of the anterior epitympanic recessus (same level as **b**, **c** and **d**) showing a rather isointense nodular lesion. No clear hyperintensity is noted

tory tissue from cholesteatoma [1, 6]. No false-positive findings have been reported in the literature, so hyperintensity on DW images can be considered diagnostic for cholesteatoma [2]. It is clear that DW EPI has a role in the visualization of the usually quite large recurrent or relapsing cholesteatoma [5–7]. Its value in the evaluation of residual cholesteatoma in pre-second-look ears, however, is limited due to the often very small size of these residual cholesteatoma pearls [2]. The size limit for visualization of an acquired middle ear cholesteatoma using DW EPI has in recent studies been set at 5 mm [2]. It is clear that smaller cholesteatoma lesions can easily be missed on DW EPI images due to the low resolution and higher slice thickness of the sequence and its sensitivity to susceptibility artifacts. This is probably the main reason why DW EPI seems to be useless for the evaluation of the usually small pre-second-look residual cholesteatoma [2]. DW EPI, however, seems to be reliable in the evaluation of the larger recurrent cholesteatoma [5–7]. Other reports have discussed the use of late post-gadolinium T1-weighted MR imaging sequence

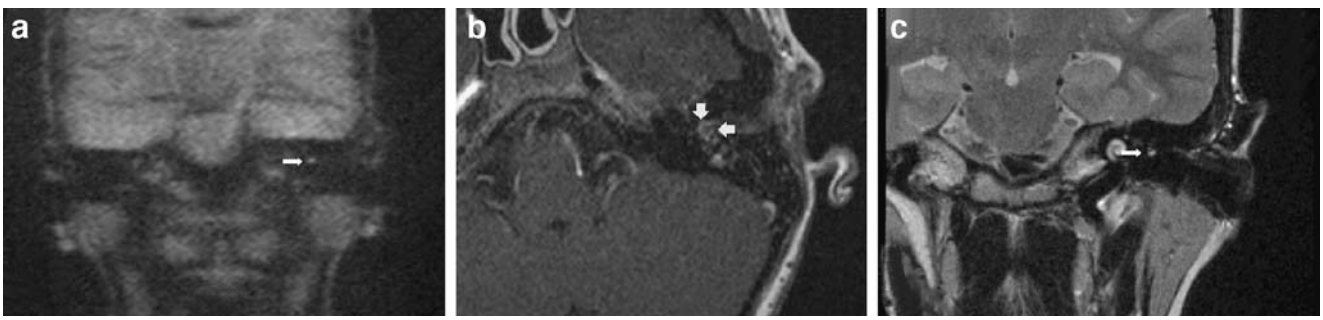

Fig. 3 Patient 3: small (2 mm) cholesteatoma, surrounded by inflammation. CT scanning was refused by the mother of the child. **a** Coronal SS TSE DW image demonstrating a very small but clearly hyperintense nodular lesion (*arrow*) in the signal void of the left middle ear. **b** Axial late post-gadolinium T1-weighted MR image with a centrally located nodular very small nonenhancing lesion (*arrows*) surrounded by enhancing tissue compatible with a very small cholesteatoma surrounded by inflammation. **c** Coronal T2-weighted image (same level as **a**) showing the very small nodular hyperintensity (*arrow*) probably situated at the mesotympanon

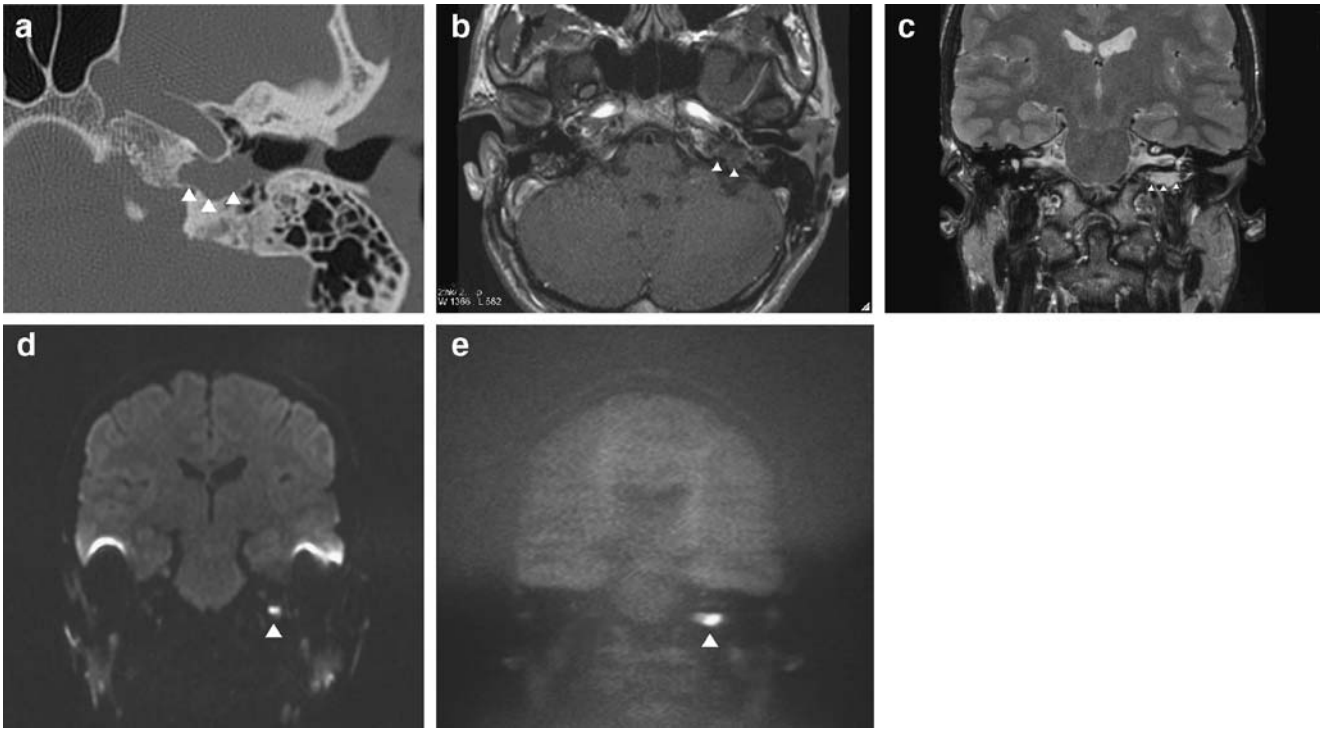

Fig. 4 Patient 7: congenital cholesteatoma in the left petrous bone. **a** Axial CT image showing a large soft-tissue lesion in the inferoposterior aspect of the temporal bone on the left side. The lesion (*arrowheads*) is in close relationship to the horizontal segment of the carotid canal. **b** Axial late post-gadolinium T1-weighted MR image (same level as **a**) showing the hypointense nonenhancing lesion posterior to the horizontal segment of the internal carotid artery (*arrowheads*). **c** Coronal T2-weighted MR image at the level of the internal auditory canal showing the moderately hyperintense congenital cholesteatoma under the internal auditory canal (*arrowheads*). **d** Coronal DW EPI image at the same level as **c**. Note the symmetrical artifacts at the interface between the temporal lobe and the temporal bone. The congenital cholesteatoma is seen as a rather small somewhat distorted nodular hyperintense lesion medial to the middle ear signal void (*arrowhead*). **e** Coronal SS TSE DW image at the same level as **c** and **d**. Note the complete lack of artifacts in this image. The cholesteatoma is seen as an oval hyperintense lesion medial to the signal void of the middle ear (*arrowheads*)

in the diagnosis of pre-second-look residual cholesteatoma [3, 4]. In the study of Williams et al. [3] the smallest cholesteatoma detected measured 2.5 mm.

Recently, two reports have discussed the use of a non-EPI-based DW sequence instead of DW EPI in the evaluation of middle ear cholesteatoma [8, 9]. Both sequences appear to be DW fast SE sequences having clearly fewer susceptibility artifacts and a higher resolution than DW EPI. Remarkably, in the study by Dubrulle et al., the size limit for detecting a recurrent cholesteatoma was set a 5 mm (equal to the size limit with the DW EPI sequence) despite the absence of artifacts and the higher resolution of the sequence [9].

In order to assess the sensitivity of this SS TSE DW MR imaging sequence in the diagnosis of cholesteatoma, we prospectively evaluated this sequence in 21 patients clinically or otoscopically strongly suspected of having a middle ear cholesteatoma, without a history of prior surgery. The aim was not to differentiate between inflammatory tissue and cholesteatoma using this SS TSE DW MR imaging sequence, as this already has been demonstrated [2], but to see what size of cholesteatoma could be detected using this sequence. For DW imaging, we used the coronal plane as it seems to result in fewer artifacts than the axial plane. This sequence uses a 180° radiofrequency refocusing pulse for each measured echo, hence reducing the susceptibility artifacts. It allows a higher imaging matrix and thinner sections (2 mm). Moreover, we combined the SS TSE DW sequence with late post-gadolinium T1-weighted sequences in the coronal and axial planes in order to see if the cholesteatoma lesions were visible on SS TSE DW images as well as on standard MR images. Furthermore, standard MR imaging sequences were used to locate the lesion in the middle ear.

Out of the 21 surgically confirmed cholesteatomas, 19 were diagnosed on SS TSE DW images. One cholesteatoma was missed by both readers (false-negative) due to the fact that the accumulated keratin (responsible for the hyperintensity on DW images) in the cholesteatoma sac had evacuated into the external auditory canal (patient 8; Fig. 1). The possibility of missing small retraction pockets or evacuated retraction pockets on DW images has been reported previously [1, 2]. Apart from this autoevacuation, a cholesteatoma can also evacuate as a result of cleaning the affected ear via the external auditory canal by the ENT surgeon. Hence, MR imaging should be performed prior to

cleaning the affected ear in order to avoid the possibility that the retained keratin has evacuated. Theoretically, the residual epithelial lining can be seen as a small enhancing line on T1-weighted images but in our patient this feature was difficult to assess because of the surrounding inflammation. Only on CT images, especially the coronal reformatted images, could the autoevacuated sac be demonstrated. It should be kept in mind that evacuation of the keratin out of the retraction pocket can cause false-negative findings.

The other false-negative finding on SS TSE DW images was caused by a small 3-mm congenital epitympanic cholesteatoma. All sequences in this examination were degraded by motion artifacts (Fig. 2). Probably these motion artifacts were responsible for misregistration of the characteristic hyperintensity of this small cholesteatoma by smearing the signal over different pixels in different slices. This caused the occurrence of, in retrospect, a small rather isointense nodule on the expected location of the cholesteatoma rather than showing a clear nodular hyperintensity (Fig. 2). However, despite the motion artifacts, one reader diagnosed this small cholesteatoma on the standard MR imaging sequences, as well on T2-weighted and late post-gadolinium T1-weighted images. Apart from this one particular case, standard T2 and late post-gadolinium T1-weighted MR imaging sequences added no information concerning the detection of the cholesteatoma. It is clear, however, that localization of the cholesteatoma was easier on standard T2- and T1-weighted MR images than on SS TSE DW images due to the fact that anatomical landmarks of the membranous labyrinth such as the internal auditory canal, vestibule, cochlea and semicircular canals were much more clearly visualized on standard MR images than on SS TSE DW images.

The lack of clear visualization of the anatomical landmarks of the temporal bone on SS TSE DW images can be regarded as one of the major drawbacks of the sequence. There is still an ongoing debate in the literature as to whether the hyperintensity of cholesteatoma is caused by diffusion restriction or secondary to a T2 shine-through effect [2]. In our series, no statistically significant difference could be found between the ADC values of cholesteatoma and gray matter in the adjacent temporal lobe. A T2 shine-through effect probably explains the hyperintensity on the SS TSE DW images. It is very striking that with this SS TSE DW sequence even a very small cholesteatoma, up to a size of 2 mm, could be visualized (Fig. 3). Other "small" cholesteatomas with a size less than or equal to 5 mm (the size limit for DW EPI) were also easily detected. It is highly probable that the lack of susceptibility artifacts, the slice thickness of 2 mm and the higher resolution allowed us to detect these small cholesteatomas. Even small cholesteatomas surrounded by inflammation were seen on SS TSE DW images as the sequence only highlights the keratin inside the cholesteatoma (Fig. 3). Late post-gadolinium T1-weighted images in patient 3 clearly demonstrated the enhancing inflammatory tissue around a very small nonenhancing cholesteatoma (Fig. 3). In this patient, surgery as well as pathology nicely demonstrated the surrounding enhancing inflammation and the centrally located 2-mm large nonenhancing cholesteatoma. Moreover, in this particular patient, CT scanning was not performed because of refusal by the mother of the child, so diagnosis was confirmed based upon only the MR imaging findings.

Although DW EPI images were also available in only five patients, the DW EPI findings compared to the SS TSE DWI findings confirmed previous reports that the size limit for detection of cholesteatoma on DW EPI seems to be 5 mm [2]. Only cholesteatomas with a size greater than 5 mm were diagnosed by both readers on DW EPI images (Fig. 4). Moreover, cholesteatomas had a distorted aspect on the DW EPI images compared to the SS TSE DWI images. We conclude that the SS TSE DWI sequence is able to detect middle ear cholesteatomas as small as 2 mm. Associating this sequence with T2-weighted and late post-gadolinium T1-weighted sequences allowed us to demonstrate surrounding inflammation and to exactly localize the lesion in the middle ear and mastoid. The fact that standard T2-weighted and late post-gadolinium T1-weighted images have no clear additional value in the detection of middle ear cholesteatoma suggests the possibility of detecting suspected middle ear cholesteatoma by starting with the SS TSE DWI sequence alone. This probably also applies to the important subgroup of postoperative ears in which detection of a residual cholesteatoma is even more important and more difficult. However, exact location of a residual cholesteatoma in postoperative ears still has to be determined with the standard sequences, including late post-gadolinium T1-weighted images, so both sequences appear to be complementary. Further studies are currently running with the aim of determining the value of the SS TSE DWI sequence in detecting and evaluating usually very small pre-second-look cholesteatomas and recurrent cholesteatomas after surgery.

Conflict of interest statement We declare that we have no conflict of interest.

References

1. Fitzek C, Mewes T, Fitzek S, Mentzel HJ, Hunsche S, Stoeter P (2003) Diffusion-weighted MRI of cholesteatoma of the petrous bone. J Magn Reson Imaging 15:636–641
2. Vercruysse JP, De Foer B, Pouillon M, Somers T, Casselman J, Offeciers E (2006) The value of diffusion-weighted MR imaging in the diagnosis of primary acquired and residual cholesteatoma; a surgical verified study of 100 patients. Eur Radiol 16:1461–1467

3. Williams MT, Ayache D, Alberti C, Heran F, Lafitte F, Elmalech-Berges M, Piekarski JD (2003) Detection of postoperative residual cholesteatoma with delayed contrast-enhanced MR imaging: initial findings. Eur Radiol 13:169–174
4. Ayache D, Wiliams MT, Lejeune D, Corre A (2005) Usefulness of delayed postcontrast magnetic resonance imaging in the detection of residual cholesteatoma in the detection of residual cholesteatoma after canal wall-up tympanoplasty. Laryngoscope 115:607–610
5. Aikele P, Kittner T, Offergeld C, Kaftan H, Huttenbrink KB, Laniado M (2003) Diffusion-weighted MR imaging of cholesteatoma in pediatric and adult patients who have undergone middle ear surgery. AJR Am J Roentgenol 181:261–265
6. Maheshwari S, Mukherji SK (2002) Diffusion-weighted imaging for differentiating recurrent cholesteatoma from granulation tissue after mastoidectomy: case report. AJNR Am J Neuroradiol 23:847–849
7. Stassola A, Magluilo G, Parrotto D, Luppi G, Marini M (2004) Detection of postoperative relapsing/residual cholesteatomas with diffusion-weighted echo-planar magnetic resonance imaging. Otol Neurotol 25:879–884
8. De Foer B, Vercruysse JP, Pilet B, Michiels J, Vertriest R, Pouillon M, Somers T, Casselman JW, Offeciers E (2006) Single-shot, turbo spin-echo, diffusion-weighted imaging versus spin-echo-planar, diffusion-weighted imaging in the detection of acquired middle ear cholesteatoma. AJNR Am J Neuroradiol 27:1480–1482
9. Dubrulle F, Souillard R, Chechin D, Vaneeclo FM, Desaulty A, Vincent C (2006) Diffusion-weighted MR imaging sequence in the detection of postoperative recurrent cholesteatoma. Radiology 238:604–610
10. Lemmerling M, De Foer B (2004) Imaging of cholesteatomatous and non-cholesteatomatous middle ear disease. In: Lemmerling M, Kollias SS (eds) Radiology of the petrous bone. Springer, Berlin, pp 31–47